환경영향평가 Vol. 29, No. 6(2020), pp.403~413 J. Environ. Impact Assess. 29(6): 403~413(2020) ISSN 1225-7184
https://doi.org/10.14249/eia.2020.29.6.403

Research Paper

Development of Optimal Chlorination Model and Parameter Studies

Joonhyun Kim · Sooyoung Ahn · Minwoo Park

Division of Architecture, Civil and Environment Engineering, Kangwon National University, Korea

최적 염소 소독 모형의 개발 및 파라미터 연구

김준현 · 안수영 · 박민우

강원대학교 공과대학 건축토목환경공학부

요약: 최적의 염소 소독 전략을 구축하기 위해 8개의 연립 준선형 편미분방정식으로 구성된 수학적 모형이 제안되었다. 다차원 수치 프로그램을 개발하기 위해 상류 가중 유한요소법을 사용하였다. 프로그램은 세 가지 유형의 반응기에서 측정된 농도에 대해 검증되었다. 16개의 실험 결과에 대해 경계 조건 및 반응 속도를 보정하여 측정된 값을 재생시켰다. 모델링 결과로부터 8개의 반응 속도계수가 추정되었다. 반응 속도계수는 pH 및 온도로 표현되었다. 반응 속도계수를 추정하기 위해 수치 오차의 제곱의 합을 최소화하는 자동 최적 알고리즘의 프로그램을 개발하고 모형에 결합하였다. 최종 사용지에서 염소 및 오염물의 농도를 최소화하기 위해서는 정수장의 염소소독공정으로부터 최종 사용지까지의 수질 변화를 모형에 의해 예측하고 이를 기반으로 유입수 수질에 따라 염소소독공정을 운영하는 실시간 예측 제어 시스템이 필요하다. 본 모형을 이용하여 정수장에 이러한 시스템을 구축할 수 있을 것이다.

주요어: 최적의 염소화 모형, 실험 및 모델링 검증, 반응 속도의 자동 추정, 다차원 유한 요소 모형, 파라미터 연구, 염소소독 모형을 이용한 예측 제어

Abstract: A mathematical model comprised with eight simultaneous quasi-linear partial differential equations was suggested to provide optimal chlorination strategy. Upstream weighted finite element method was employed to construct multidimensional numerical code. The code was verified against measured concentrations in three type of reactors. Boundary conditions and reaction rate were calibrated for the sixteen cases of experimental results to regenerate the measured values. Eight reaction rate coefficients were estimated from the modeling result. The reaction rate coefficients were expressed in terms of pH and temperature. Automatic optimal algorithm was invented to estimate the reaction rate coefficients by minimizing the sum of squares of the numerical errors and combined with the model. In order to minimize the concentration of chlorine and pollutants at the final usage sites, a real-

First Author: Joonhyun Kim, Tel: +82-33-250-6354, E-mail: joonhkim@kangwon.ac.kr, ORCID: 0000-0002-9666-5570
Corresponding Author: Sooyoung Ahn, Tel: +82-33-250-6354, E-mail: asy0716@nate.com, ORCID: 0000-0001-8685-7619
Co-Author: Minwoo Park, Tel: +82-33-250-2921, E-mail: pmw0628@rig.re.kr, ORCID: 0000-0003-3672-269X
Received: 7 July, 2020. Revised: 18 November, 2020. Accepted: 2 December, 2020.

time predictive control system is imperative which can predict the water quality variables from the chlorine disinfection process at the water purification plant to the customer by means of a model and operate the disinfection process according to the influent water quality. This model can be used to build such a system in water treatment plants.

Keywords : Optimal chlorination model, experimental and modeling verification, automatic estimation of reaction rate, multidimensional finite element model. parameter study, predictive control system of chlorination model

I. Intordution

Despite the widespread acceptance of chlorine as a water and wastewater disinfectant, the by-product of chlorinated organic compounds, such as THMs, has become a particularly bothersome aspect of chlorination. The goal of this study is to develop an optimal chlorination method through the improved understanding of reaction kinetics in dispersed flow reactors in water and wastewater treatment plants. The dynamics of breakpoint chlorination were examined in three continuous dispersed flow reactors (Stenstrom and Tran, 1984). Figure 1 shows the process flow and instru-

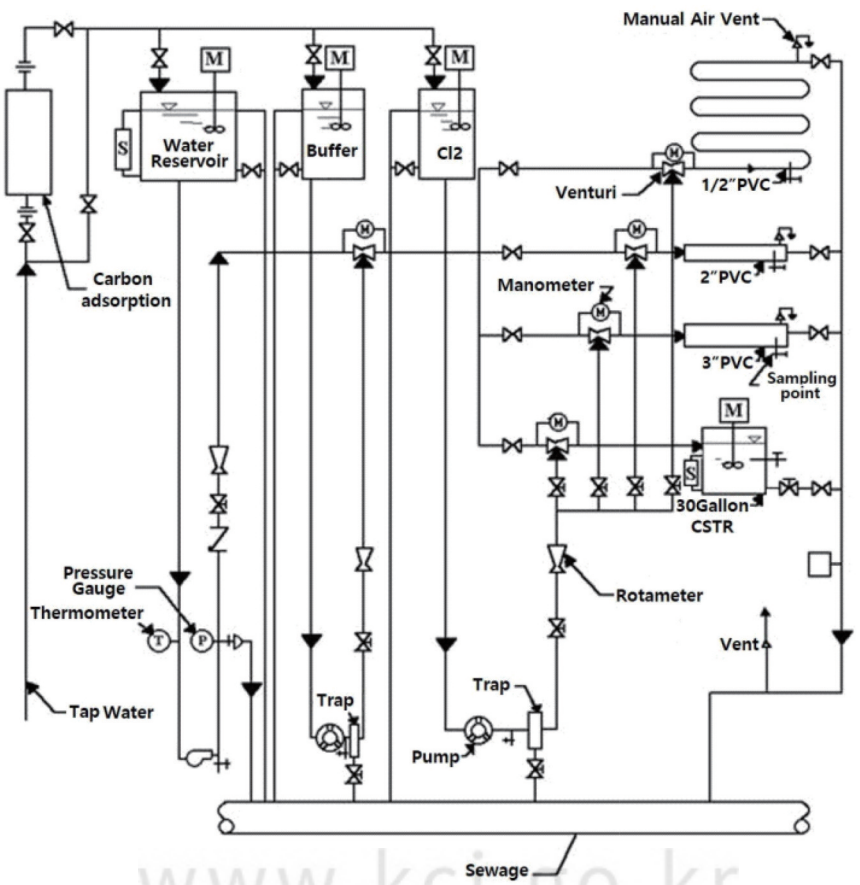

Figure 1. Process flow and instrumentation diagram of the pilot plant (Stenstrom and Tran, 1984).

mentation diagram for that pilot plant. The reactors were comprised of 1/2, 2 and 3 inch PVC pipe, which were 730, 41, and 23 feet long, respectively.

Chlorination of ammonia at various chlorine to ammonia ratios were investigated over the pH range of 6.5 to 7.5. Seventeen experiments were performed over the course of the investigations. Chlorine residuals, including free, monochloramine, dichloramine, and nitrogen trichloride, and ammonia were analyzed simultaneously. From the results of these experiments more fundamental understanding of chlorination dynamics was acquired.

To quantitatively characterize the breakpoint reactions, mathematical models, consisting of eight simultaneous, quasi-linear, partial differential equations were developed. The models were solved by using a multidimensional finite element method (Kim, 1995, 2018). The reaction rate coefficients were treated as parameters, and were estimated using a search technique to minimize the sum of squares of the difference between the expected and measured values. Model predictions and experimental results agreed well. This study was initiated as a continuous effort to develop process operating strategies to maximize or minimize any given experimental objectives. The specific technical goal and accomplishments of this study can be summarized as follows:

1) Development of mathematical model describing the breakpoint chlorination reactions.
2) Verification of the mathematical model against experimental data.
3) Improvement of numerical techniques for multidimensionality and complex boundary conditions by using multdimensional finite element method (Kim, 1995, 2018).
4) Improved estimation of kinetic parameters of the previous works (Wei, 1972, Stenstrom and Tran, 1984).
5) Practical conceptualization of improved chlorination for the minimization of toxic byproducts.

II. Dynamic Model for Breakpoint Chlorination

1. Breakpoint kinetics and mechanisms

The breakpoint reaction mechanism in this study is shown in Figure 2 and the theoretical reaction rate is expressed in Table 1.

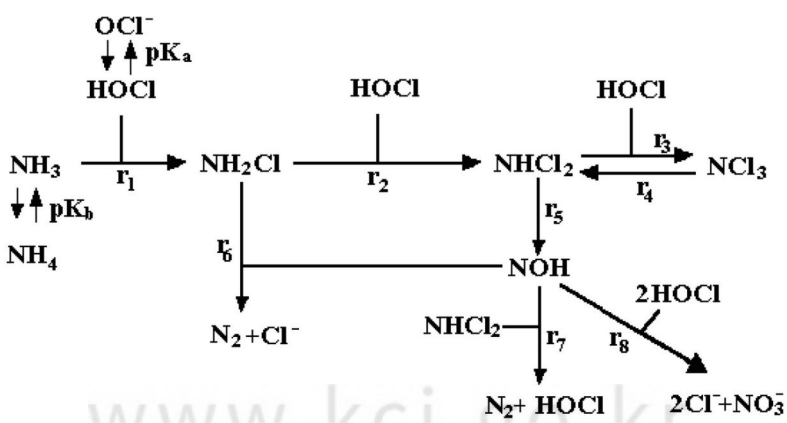

Figure 2. Breakpoint mechanism of Wei (1972).

Table 1. Theoretical reaction rate and relevant breakpoint reactions

Breakpoint Reactions	Reaction Rate	Components
$HOCl + NH_3 \rightarrow NH_2Cl + H_2O$	$r_1 = k_{10}CN$	$C = [HOCl] + [OCl^-]$
$HOCl + NH_2Cl \rightarrow NHCl_2 + H_2O$	$r_2 = k_{20}CM$	$N = [NH_3] + [NH_4^+]$
$HOCl + NHCl_2 \rightarrow NCl_3 + H_2O$	$r_3 = k_{30}CD$	$M = [NH_2Cl]$
$NCl_3 + H_2O \rightarrow NHCl_2 + HOCl$	$r_4 = k_{40}E$	$D = [NHCl_2]$
$NHCl_2 + H_2O \rightarrow NOH + 2H^+ + 2Cl^-$	$r_5 = k_{50}D$	$E = [NCl_2]$
$NOH + NH_2Cl \rightarrow N_2 + H_2O + H^+ + Cl^-$	$r_6 = k_{60}SM$	$S = [NOH]$
$NOH + NHCl_2 \rightarrow N_2 + HOCl + H^+ + Cl^-$	$r_7 = k_{70}SD$	$G = [N_2]$
$NOH + 2HOCl \rightarrow NO_3 + 3H^+ + 2Cl^-$	$r_8 = k_{80}SC$	$I = [NO_2^-]$

Table 2. Initial trial values of reaction rate coefficients

Theoretical coefficients by Wei	Theoretical coefficients in this Study	Observed coefficients by Wei	Observed coefficients in this Study
$k_1 = 9.7 \times 10^8 \times e^{(-3000/RT)}$	$k_1 = 9.7 \times 10^8 \times e^{(-3000/RT)}$	$k_{10} = \frac{k_1}{\left[1+\frac{k_a}{[H^+]}\right]\left[1+\frac{k_b[H^+]}{K_w}\right]}$	$k_{10} = \frac{k_1}{\left[1+\frac{k_a}{[H^+]}\right]\left[1+\frac{k_b[H^+]}{K_w}\right]}$
$k_2 = 2.43 \times 10^4 \times e^{(-2400/RT)}$	$k_2 = 2.43 \times 10^4 \times e^{(-2400/RT)}$	$k_{20} = k_2 / \left[1+\frac{k_a}{[H^+]}\right]$	$k_{20} = k_2 / \left[1+\frac{k_a}{[H^+]}\right]$
$k_3 = 8.75 \times 10^{10} \times e^{(-3800/RT)}$	$k_3 = 3.43 \times 10^5 \times e^{(-7000/RT)}$	$k_{30} = k_3[H^+] / \left[1+\frac{k_a}{[H^+]}\right]$	$k_{30} = k_3 / \left[1+\frac{k_a}{[H^+]}\right]$
$k_4 = 6.32 \times 10^{11} \times e^{(-13000/RT)}$	$k_4 = 3 \times 10^{10} \times e^{(-20,000/RT)}$	$k_{40} = k_4[H^+]$	$k_{40} = k_4$
$k_5 = 2.11 \times 10^{10} \times e^{(-7200/RT)}$	$k_5 = 2.03 \times 10^{14} \times e^{(-7200/RT)}$	$k_{50} = k_5[OH^-]$	$k_5 = k_5$
$k_6 = 5.53 \times 10^7 \times e^{(-3000/RT)}$	$k_6 = 5 \times 10^7 \times e^{(-6000/RT)}$	$k_{60} = k_6$	$k_{60} = k_6$
$k_7 = 6.02 \times 10^8 \times e^{(-6000/RT)}$	$k_7 = 6 \times 10^8 \times e^{(-6000/RT)}$	$k_{70} = k_7$	$k_{70} = k_7$
$k_8 = 7.18 \times 10^7 \times e^{(-6000/RT)}$	$k_8 = 5 \times 10^7 \times e^{(-6000/RT)}$	$k_{80} = k_8 / \left[1+\frac{k_a}{[H^+]}\right]$	$k_{80} = k_8 / \left[1+\frac{k_a}{[H^+]}\right]$

Before estimating the reaction rate coefficients by modeling, the theoretical reaction rate coefficients and the experimental reaction rate coefficients were compared in Table 2 below to obtain the initial values for the estimation of the reaction rate coefficients.

The observed reaction rate coefficients were derived from the theoretical coefficients as shown in Table 2, which is different from the Wei's rate. In the case of dichloramine and trichloramine, pH influence is stronger in Wei's formulation.

2. Mathematical formulation of Multidimensional Finite Element Model

The mass transport equation is combined with the breakpoint reactions in Figure 2 to produce a set of eight nonlinear partial differential equations. These equations can predict the concentration of all major chlorine species. The typical form of these equation is as follows:

$$\frac{\partial C_i}{\partial t} = \Delta(\boldsymbol{D}\Delta C_i) - \Delta(\vec{V}C_i) + kC^*C_i + S_i = \Delta(\boldsymbol{D}\Delta C_i) - \Delta(\vec{V}C_i) + R_i$$

The eight nonlinear partial differential equations are as follows:

$$\frac{\partial C}{\partial t} = \frac{\partial}{\partial x}(D\frac{\partial C}{\partial x}) - V\frac{\partial C}{\partial x} - r_1 - r_2 - r_3 + r_4 + r_7 - 2r_s$$

$$\frac{\partial N}{\partial t} = \frac{\partial}{\partial x}(D\frac{\partial N}{\partial x}) - V\frac{\partial N}{\partial x} - r^1,$$

$$\frac{\partial M}{\partial t} = \frac{\partial}{\partial x}(D\frac{\partial M}{\partial x}) - V\frac{\partial M}{\partial x} + r_1 - r_2 - r_6$$

Table 3. Separation of reaction and source terms

Overall Reaction Terms	Quasilinear Reaction Coefficients	Source Terms
$R_1 = -r_1 - r_2 - r_3 + r_4 + r_7 - 2r_s$	$kC^* = -k_{10} \times C_2 - k_{20} \times C_3 - k_{30} \times C_4 - 2k_{80} \times C_5$	$s = k_{40} \times C_8 + k_{70} \times C_4 \times C_5$
$R_2 = -r_1$	$kC^* = -k_{10} \times C_1$	$s = 0$
$R_3 = r_1 - r_2 - r_6$	$kC^* = -k_{20} \times C_1 - k_{60} \times C_5$	$s = k_{10} \times C_1 \times C_2$
$R_4 = r_2 - r_3 + r_4 - r_5 - r_7$	$kC^* = -k_{30} \times C_2 - k_{50} - k_{70} \times C_5$	$s = k_{20} \times C_1 \times C_3 + k_{40} \times C_5$
$R_5 = r_5 - r_6 - r_7 - r_8$	$kC^* = -k_{60} \times C_3 - k_{70} \times C_4 - 2k_{80} \times C_1$	$s = k_{50} \times C_4$
$R_6 = r_6 + r_7$	$kC^* = 0$	$s = k_{60} \times C_3 \times C_5 + k_{70} \times C_4 \times C_5$
$R_7 = r_8$	$kC^* = 0$	$s = 2k_{80} \times C_1 \times C_5$
$R_8 = r_3 - r_4$	$kC^* = -k_{40}$	$s = k_{30} \times C_1 \times C_4$

$$\frac{\partial D}{\partial t} = \frac{\partial}{\partial x}(D\frac{\partial D}{\partial x}) - V\frac{\partial D}{\partial x} + r_2 - r_3 + r_4 - r_5 - r_7$$

$$\frac{\partial S}{\partial t} = \frac{\partial}{\partial x}(D\frac{\partial S}{\partial x}) - V\frac{\partial S}{\partial x} + r_5 - r_6 - r_7 - r_8,$$

$$\frac{\partial G}{\partial t} = \frac{\partial}{\partial x}(D\frac{\partial G}{\partial x}) - V\frac{\partial G}{\partial x} + r_6 + r_7$$

$$\frac{\partial I}{\partial t} = \frac{\partial}{\partial x}(D\frac{\partial I}{\partial x}) - V\frac{\partial I}{\partial x} + r_8,$$

$$\frac{\partial E}{\partial t} = \frac{\partial}{\partial t}(D\frac{\partial E}{\partial x}) - V\frac{\partial E}{\partial x} + r_3 - r_4$$

The reaction kinetics of the above chlorination process is systematically defined as shown in Table 3 to facilitate the coding.

The finite element analogue is derived as follows by using the finite element modules for the evaluation of spatial derivatives of the governing equation (Kim, 1995).

$$\sum_{e=i}^{nel}\Big[\Big\{\frac{1}{\Delta t}[ET] + \varepsilon([EV] + [ED] - kC^*[ET])\Big\}\{C_i^{n+1}\}$$
$$= \Big\{\frac{1}{\Delta t}[ET] + (\varepsilon - 1)([EV] + [ED] - kC^*[ET])\Big\}\{C_i^n\}$$
$$+ [ET]\{S_i\} + \{f_i\}\Big]$$

Where, [ET], [EV], [ED] are the element matrices with respect to time derivative, velocity, and dispersive flux terms, which depend on known parameters and coordinates.

$$ET_{i,j} = <W_i, N_j> = \int\int\int W_i N_j \, dxdydz =$$
$$\int\int\int W_i N_j |J| d\xi d\eta d\zeta = \sum_{ig=1}^{nn} W_{i,ig} N_{j,ig} |J|$$

$$EV_{jd,ij} = <W_i, \frac{dN_j}{dx_{jd}}> = \sum_{ig=1}^{nn} W_{i,ig} \frac{dN_{j,ig}}{dx_{jd}} |J|$$

$$ED_{id,jd,i,j} = <\frac{dW_j}{dx_{id}}, \frac{dN_j}{dx_{jd}}> = \sum_{ig=1}^{nn} \frac{dW_{i,ig}}{dx_{id}} \frac{dN_{j,ig}}{dx_{jd}} |J|$$

3. Automatic estimation of the reaction rate coefficients

The parameter estimation algorithm requires the sequential estimation and linearization of the objective function around an initial set of parameter estimates. By perturbing each parameter and observing the effect on the objective function, a new set of parameter estimates can be obtained which minimizes the sum of squares error of the linearized model. The model can then be solved with the new set of parameters, and a new set of perturbations can be made. This procedure can be repeated until further perturbations provide no improvement in the objective function.

The weighted least squares criterion was used as the objective function as follows:

$$Min\ J = W_C \sum_i \sum_j (\alpha_i^j)^2 + W_M \sum_i \sum_j (\beta_i^j)^2 + W_D \sum_i \sum_j (\delta_i^j)^2 +$$
$$W_E \sum_i \sum_j (\xi_i^j)^2 + W_N \sum_i \sum_j (\mu_i^j)^2 + W_P \sum_i \sum_j (\eta_i^j)^2$$

over k_2, k_3, k_4, k_5, k_6, k_7, k_8

Where $\alpha_i^j = C_i^j - C_i^{*j}$, $\beta_i^j = M_i^j - M_i^{*j}$, $\delta_i^j = D_i^j - D_i^{*j}$, $\xi_i^j = E_i^j - E_i^{*j}$, $\mu_i^j = N_i^j - N_i^{*j}$, $\eta_i^j = P_i^j - P_i^{*j}$, i the sample location number, and j is the observation time. C_i^{*j}, M_i^{*j}, D_i^{*j}, E_i^{*j}, N_i^{*j} are the measured values, and C_i^j, M_i^j, D_i^j, E_i^j, N_i^j are the modeling results.

At time j, and for sampling point I, P is the molar ratio of chlorine reduced to ammonia oxidized.

$$P_i^j = \frac{C_{iniitial} - (C_i^j + M_i^j + D_i^j + E_i^j)}{N_{initial} - N_i^j},$$

$$P_i^{*j} = \frac{C_{iniitial} - (C_i^{*j} + M_i^{*j} + D_i^{*j} + E_i^{*j})}{N_{initial} - N_i^{*j}}$$

4. Verification of numerical stability and accuracy

Existing computational models for mass transport problems have a big problem at the area of rapidly changing concentration due to advective dominant flux, near a pollution source, or a spatially abrupt change in model parameters. This problem has been recognized as a chronic problem in the development of numerical models for environmental pollution. Many studies have been conducted over the past 30 years and various techniques have been developed. Among these, representative methods are upstream weighting method, particle tracking method, average characteristic method, and Eulerian-Lagrangian method.

Such numerical instability can lead to very serious results in the case of nonlinear problems, and solutions may diverge, show erratic results, or fail to derive solutions. Therefore, chlorine disinfection, the subject of this paper, is a very strong

Table 4. Input data for numerical stability analysis of MFEMCL

File	Model	Dispersive Co.	Velocity	Time Weighting Factor	Upstream Weighting Factor
fcs11	MFEMCL	0.0001725	0.369	0.67	-0.03
fw14	MFEMWASP	0.0001725	0.369	0.67	-0.03
fcs12	MFEMCL	0.001725	0.369	0.67	-0.03
fw15	MFEMWASP	0.001725	0.369	0.67	-0.03
fcs13	MFEMCL	0.01725	0.369	0.67	-0.03
fw16	MFEMWASP	0.01725	0.369	0.67	-0.03

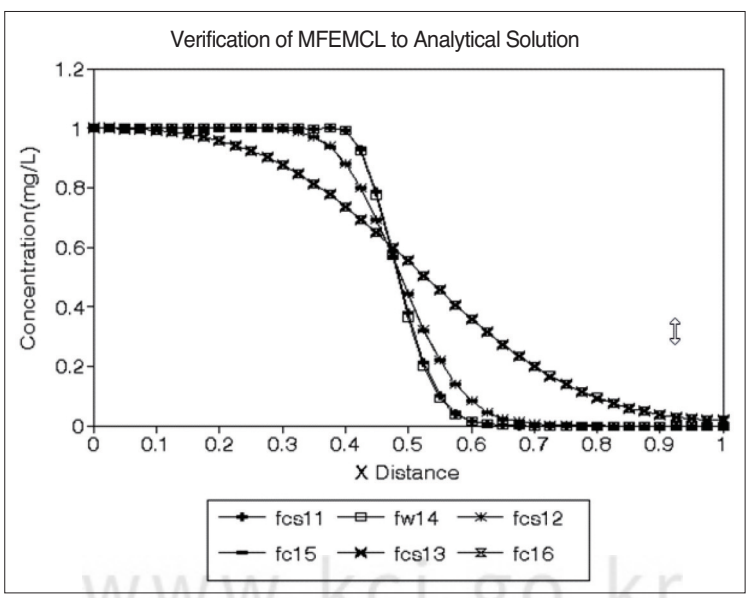

Figure 3. Computational result of MFEMCL for numerical stability analysis.

nonlinear problem in which eight substances interact with each other, so it is very important to be sure of the ability of the model to solve this instability problem. For this verification, the results of MFEMWASP (Multidimensional Finite Element Model with WASP Kinetics) were compared with MFEMCL (Multidimensional Finite Element Model for Chlorination) for three problems in the case of very strong flow rate, medium case, and strong diffusion (Kim, 1995, 2018). MFEMWASP is a model previously developed for eutrophication analysis. Kim (1995) compared the one-dimensional solute transport problem with analytical and numerical solutions in order to analyze the numerical stability of the eutrophication model. The characteristics of the comparative data are shown in Table 4, and the modeling results are shown in Figure 3.

III. Modeling Results and Reaction Rate Coefficients

Numerical stability has been verified against advective dominant migration problem in one-dimensional space. The modeling results showed good agreement with the analytical solutions. Using this stable code, applicability test was implemented using the 16 sets of experimental data of Stenstrom and Tran (1984). Even though Stenstrom performed automatic parameter estimation in 1984, the fluctuation of reaction parameter was so severe that it was very difficult to derive the parameters of Arrehnius equation from the simulation result. To overcome this problem, parameter values were varied according to the Arrehnius equation, and boundary conditions were calibrated based upon the characteristics of each data (Table 5).

The modeling results showed good agreement with measured data (Figure 4 – 6).

Table 5. Calibration of boundary conditions and reaction rate coefficients

File Name	pH	Boundary Conditions				Reaction Rate Coefficients		
		Free Chl.	Ammonia	Mono.	Di	k10	k20	k30
fc11	6.10	5.27	0.95	4.68	1.02	1.50E-03	2.30E-03	1.84E-04
fc12	7.20	0.70	0.90	4.20	0.00	1.13E-03	1.23E-03	1.34E-04
fc21	6.14	6.27	0.95	4.68	1.02	1.50E-03	2.99E-03	1.83E-04
fc22	6.80	5.48	0.95	3.02	0.00	1.37E-03	2.66E-03	3.63E-04
fc23	7.03	4.20	0.95	2.90	0.00	1.25E-03	1.42E-03	5.48E-04
fc24	8.20	4.20	0.99	3.50	0.00	3.11E-04	3.01E-04	5.69E-04
fc31	6.05	6.27	0.95	4.68	1.02	1.50E-03	3.00E-03	1.80E-04
fc32	7.00	4.20	0.98	3.00	0.00	1.26E-03	1.23E-03	5.51E-04
fc33	7.47	4.50	0.90	2.00	0.00	9.01E-04	8.75E-04	1.50E-03
fc34	7.00	5.00	0.92	2.00	0.00	1.26E-03	1.23E-03	1.50E-03
fc35	6.04	6.27	0.92	4.58	1.00	1.50E-03	3.00E-03	1.60E-04
fc36	6.50	4.27	0.94	3.60	0.68	1.20E-03	2.83E-03	1.45E-04
fc37	6.75	4.27	0.94	2.50	1.02	1.26E-03	2.70E-03	1.63E-03
fc38	7.15	3.20	0.98	2.00	0.00	1.17E-03	1.11E-03	1.59E-03
fc39	7.44	3.50	0.92	1.50	0.00	9.28E-04	9.01E-04	1.50E-03
fc310	7.65	4.00	0.90	2.20	0.00	5.60E-04	5.43E-04	1.56E-03

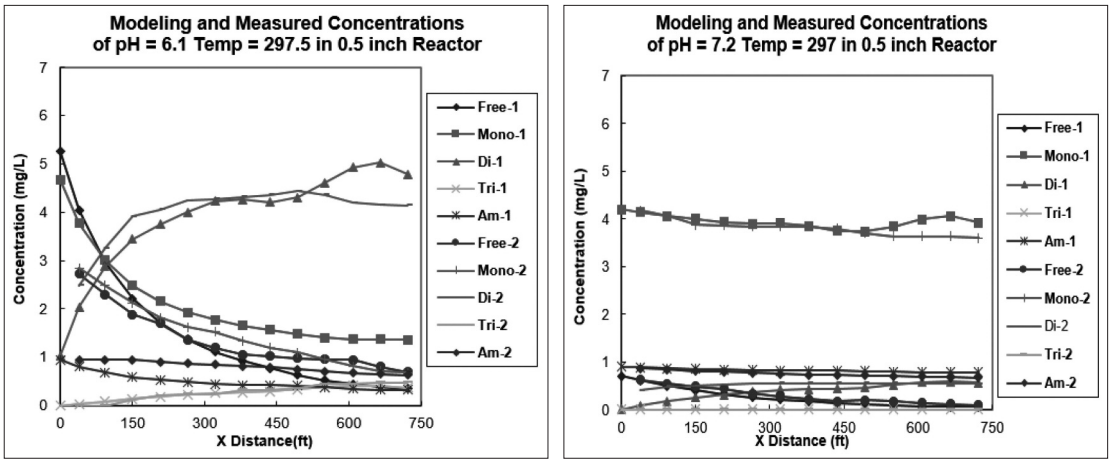

Figure 4. Modeling and measured concentrations in 0.5 inch reactor : fc11 & fc12.

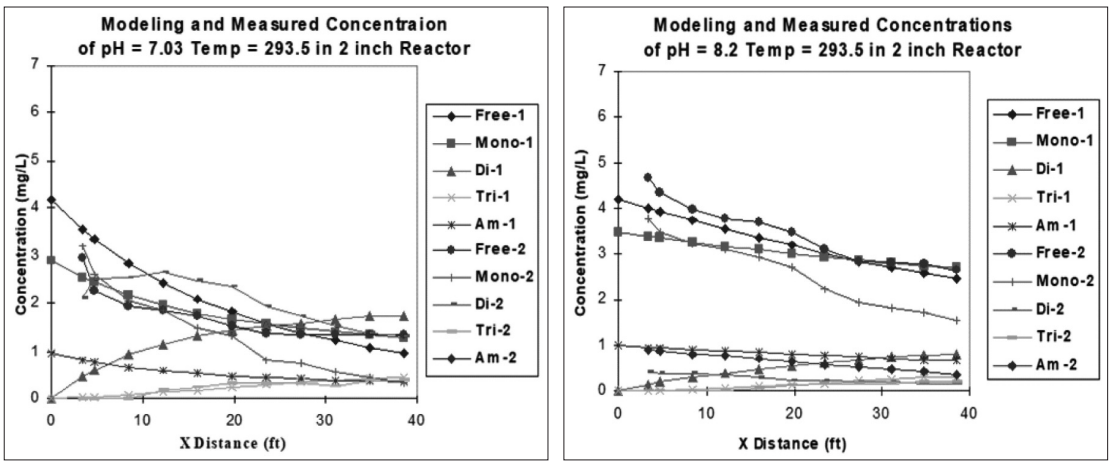

Figure 5. Modeling and measured concentrations in 2 inch reactor : fc23 & fc24.

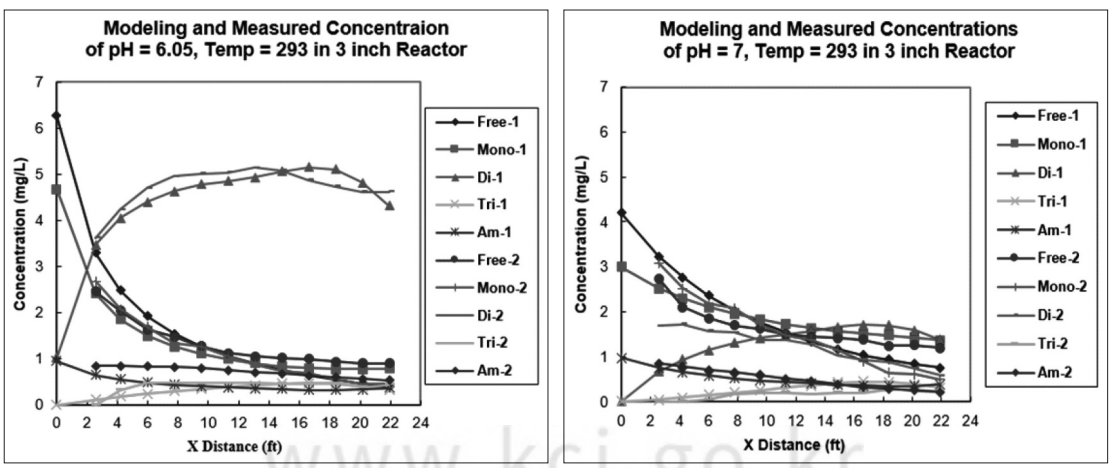

Figure 6. Modeling and measured concentrations in 3 inch reactor : fc31 & fc32.

The variation of reaction rate coefficient is shown in Table 6. Because each reactor has different sampling points, variable grids were constructed to coincide the computational points as shown in Table 7. Final form of the theoretical reaction rate coefficients is shown in Table 8.

The calibration and estimation procedure of the reaction rate coefficients resulted specific findings as follows:

1) The proposed method in this study is most appropriate near pH 6 range.
2) It was difficult to calibrate the model near the high and low pH values.
3) Dichloramine showed distinct variation with pH. The value of k20 should be reduced twice the pH variation.
4) k10 and k30 were easily estimated within Arrehnius theory.

Table 6. Estimation of reaction rate coefficients from a series of modeling results

	Arrhenius Constants					pOH-pKb	alpha	beta	k10=k1	k20=k2 /alpha	k30=k3
pKa	A0	B0	ki=A0/exp (B0/RT)	pH	pH-pKa	14-pH-pKb	1+10^ (pH-pKa)	1+10^ (pOH-pKb)	/alpha /beta	/alpha	/alpha
7.582	1.60E-03	3	1.60E-03	0	-7.582	4.599	1.00E+00	3.97E+04	4.03E-08	3.10E-03	1.90E-04
	3.10E-03	2.4	3.10E-03	1	-6.582	3.599	1.00E+00	3.97E+03	4.03E-07	3.10E-03	1.90E-04
	1.90E-04	3.8	1.90E-04	2	-5.582	2.599	1.00E+00	3.98E+02	4.02E-06	3.10E-03	1.90E-04
pKb	1.00E+00	1.3	1.00E+00	3	-4.582	1.599	1.00E+00	4.07E+01	3.93E-05	3.10E-03	1.90E-04
9.401	1.00E+00	7.2	1.00E+00	4	-3.582	0.599	1.00E+00	4.97E+00	3.22E-04	3.10E-03	1.90E-04
	1.00E+00	3	1.00E+00	5	-2.582	-0.401	1.00E+00	1.40E+00	1.14E-03	3.09E-03	1.90E-04
	1.00E+00	6	1.00E+00	6	-1.582	-1.401	1.03E+00	1.04E+00	1.50E-03	3.02E-03	1.85E-04
	1.00E+00	6	1.00E+00	6	-1.542	-1.441	1.03E+00	1.04E+00	1.50E-03	3.01E-03	1.85E-04
				6.1	-1.532	-1.451	1.03E+00	1.04E+00	1.50E-03	3.01E-03	1.85E-04
				6.1	-1.482	-1.501	1.03E+00	1.03E+00	1.50E-03	3.00E-03	1.84E-04
				6.1	-1.442	-1.541	1.04E+00	1.03E+00	1.50E-03	2.99E-03	1.83E-04
				6.5	-1.082	-1.901	1.08E+00	1.01E+00	1.46E-03	2.86E-03	1.75E-04
				6.8	-0.832	-2.151	1.15E+00	1.01E+00	1.38E-03	2.70E-03	1.66E-04
Temp				6.8	-0.782	-2.201	1.17E+00	1.01E+00	1.36E-03	2.66E-03	1.63E-04
293				7	-0.582	-2.401	1.26E+00	1.00E+00	1.26E-03	2.46E-03	1.51E-04
				7	-0.552	-2.431	1.28E+00	1.00E+00	1.24E-03	2.42E-03	1.48E-04
				7.2	-0.432	-2.551	1.37E+00	1.00E+00	1.16E-03	2.26E-03	1.39E-04
				7.2	-0.382	-2.601	1.41E+00	1.00E+00	1.13E-03	2.19E-03	1.34E-04
				7.4	-0.142	-2.841	1.72E+00	1.00E+00	9.28E-04	1.80E-03	1.10E-04
				7.5	-0.112	-2.871	1.77E+00	1.00E+00	9.01E-04	1.75E-03	1.07E-04
				7.9	0.268	-3.251	2.85E+00	1.00E+00	5.60E-04	1.09E-03	6.66E-05
				8	0.418	-3.401	3.62E+00	1.00E+00	4.42E-04	8.57E-04	5.25E-05
				8.2	0.618	-3.601	5.15E+00	1.00E+00	3.11E-04	6.02E-04	3.69E-05
				9	1.418	-4.401	2.72E+01	1.00E+00	5.89E-05	1.14E-04	6.99E-06
R				10	2.418	-5.401	2.63E+02	1.00E+00	6.09E-06	1.18E-05	7.23E-07
1987				11	3.418	-6.401	2.62E+03	1.00E+00	6.11E-07	1.18E-06	7.25E-08
				12	4.418	-7.401	2.62E+04	1.00E+00	6.11E-08	1.18E-07	7.26E-09
				13	5.418	-8.401	2.62E+05	1.00E+00	6.11E-09	1.18E-08	7.26E-10
				14	6.418	-9.401	2.62E+06	1.00E+00	6.11E-10	1.18E-09	7.26E-11

Table 7. Numerical and physical data of simulation for each reactor

Data	Input Data for Different Reactors						
	dx	nel	dt	tmax	Velocity	Dispersion	Flow Rate
fc11	1.88	262	60	600	1.635	0.112	1
	2.86	262	60	600	1.635	0.112	1
	2.86	262	60	600	1.635	0.112	1
fc21	0.1785	233	60	600	0.102	0.0245	1
	0.0561	233	60	600	0.102	0.0245	1
	0.1887	233	60	600	0.102	0.0245	1
fc31	0.1316	251	60	600	0.045	0.002	1
	0.0863	251	60	600	0.045	0.002	1
	0.0885	251	60	600	0.045	0.002	1
fc35	0.1316	251	60	600	0.045	0.002	0.6
	0.0863	251	60	600	0.045	0.002	0.6
	0.0885	251	60	600	0.045	0.002	0.6

Table 8. Final form of theoretical reaction rate coefficients

Parameters	Theoretical Reaction Coefficients	Usage
k_1	$1.6 \times 10^{-3} \times$ exponential (-3.0/RTk)	Monochloramine Production
k_2	$3.1 \times 10^{-3} \times$ exponential (-2.4/RTk)	Dichloramine Production
k_3	$1.9 \times 10^{-4} \times$ exponential (-3.8/RTk)	Trichloramine Production

5) Final estimation of theoretical reaction rate coefficient k1, k2, k3 are shown in Table 8.
6) The difference between the final form of Arrehnius constant and the conventional value arises from the facts that (1) the experiment was performed in dispersive flow reactor, not in batch reactor, and (2) the confidence of experiment were increased with the iterative 16 experiments. Within pH 6 range, consistent variation pattern was observed both in experimental and modeling results
7) During the conversion process of theoretical reaction rate to observed rate, pH has strong impact. Thus, in this study the equations of the observed reaction rate were derived as shown in Table 2. However, according to the measured concentration of dichloramine and monochloramine, pH has strong influence than the derived equation. The cause of this phenomenon might be inappropriate Morris system or unknown reactions.
8) To get precise result of the modeling, it is imperative to measure the boundary concentration right after the injection point of chlorine.

IV. Conclusions and Future Works

For the optimal chlorination strategy, finite element code was developed based upon eight simultaneous breakpoint reactions. The code was verified against the convective dominant flux system and the measured concentrations in three types of reactors. Specific Arrehnius constant was estimated from these modeling and experimental technique. The proposed reaction rate coefficients might be suitable for the use of normal operation condition in water treatment plant, which was

expressed in terms of pH and temperature. The developed model MFEMCL can be used to simulate continuous flow chlorination process to maximize any operational strategies in water treatment plant or any given experimental objectives. Especially, with this portable program and expert system, automatic and optimal operation of water treatment plant can be provided in near future.

References

Kim JH. 1995. A Multidimensional finite element model for eutrophication and thermal pollution problem. Proceeding of the International Joint Seminar. Seoul National University.

Kim JH. 2018. Development and Verification of Numerical Model for Optimal Chlorination in Water Treatment Plant. Good and Justice Pub..

Stenstrom MK, Tran HG. 1984. A Theoretical and Experimental Investigation of the Dynamics of Breakpoint Chlorination in Dispersed Flow Reactors. UCLA-ENG-84-30.

Wei IWT. 1972. Chlorine-Ammonia, Breakpoint Reaction: Kinetics and Mechanism. Doctoral Dissertation in Sanitary Engineering. Harvard University.